ANNALS of Faculty Engineering Hunedoara – International Journal of Engineering
Tome XX [2022] | Fascicule 4 [November]

[1.]Aida BALTAG, [1.]Gheorghe LIVINT, [1.]Alina Georgiana BACIU

# ROBUST CONTROL STRUCTURES FOR WIND TURBINES BASED ON DFIG

[1.]"Gheorghe Asachi" Technical University of Iasi, ROMANIA

**Abstract:** This paper presents some aspects of robust control structure of DFIG-based wind turbine: drivetrain control and doubly fed induction generator control. Models of horizontal axis wind turbines and the theoretical principles of robust control that provides high performances under model uncertainties is presented. For the drivetrain, a state-space model is used to determine the transfer functions. For the induction generator, a vector control structure with stator flux orientation has adopted. An H-infinity controller is proposed for the drivetrain presents and a fractional order proportional integral controller (FOPI) is proposed for control the generator currents. With these controllers, high performances is obtained compared to conventional proportional integral controllers (PI) in the presence of external disturbances, measurement noises and turbine parameter variations. This paper an H-infinity controller and fractional order controller design methods presents. Comparative results of simulations, realized in Matlab-Simulink, are presented and include the control of the drivetrain with H-infinity controller and PID controller and the vector control of DFIG with a FOPI controller and a conventional PI controller.

**Keywords:** wind turbine, doubly fed induction generator, robust control, $\mathbf{H}_\infty$ controller, fractional-order proportional integral controller

## 1. INTRODUCTION

In the conditions of decreasing fossil fuel supplies and climate change, electricity production based on the use of renewable resources has developed in recent years. The most popular renewable energy sources are: wind energy, solar energy, wave energy, geothermal energy [12], [17]. Electricity production from wind energy is constantly growing, currently accounting for about 20% of European electricity consumption. The increase in wind power generation has also been supported by increasing the power of wind turbines from 1.5 MW, 2 MW to 5MW [18] and by improving control strategies [4], [5], [20]. In variable speed wind turbines, doubly fed induction generators are frequently used due to low cost, high efficiency and low noise [2], [11], [12].

The principle of the doubly fed induction generator is that the stator windings are connected directly to the grid, and the rotor windings are connected to the constant frequency grid via two bidirectional power converters. The power converters handle only a part of the power supplied by the turbine (nearby 30%) [2], [11]. In this paper, a design method for an H-infinity controller [11], [14], [19] and fractional order controller is presented and analyzed. The two controllers are designed for the drivetrain (H-infinity control), respectively for current control (fractional order controller), highlighting the necessary conditions for determining their parameters.

## 2. WIND TURBINE WITH DFIG MODEL

The configuration of a horizontal axis wind turbine with a doubly fed induction generator is shown in Figure 1. The bidirectional, voltage and frequency, $\mathbf{AC/DC/AC}$ converter is used to achieve the bidirectional power flow between rotor and grid and is divided to two components: the rotor-side converter, denoted $\mathbf{C_{rotor}}$ and the grid-side converter, denoted $\mathbf{C_{grid}}$. A large capacitor, $\mathbf{C}$, is connected on the $\mathbf{DC}$ side and acts as a constant voltage source, while a coupling inductor $\mathbf{L}$ connects the $\mathbf{C_{grid}}$ converter to the grid. The three-phase rotor windings are connected to the $\mathbf{C_{rotor}}$ converter by slip rings and brushes, and the three-phase stator windings are connected directly to the grid. The speed control and the active and reactive power flow control between generator and grid are achieved by controlling the bidirectional converter.

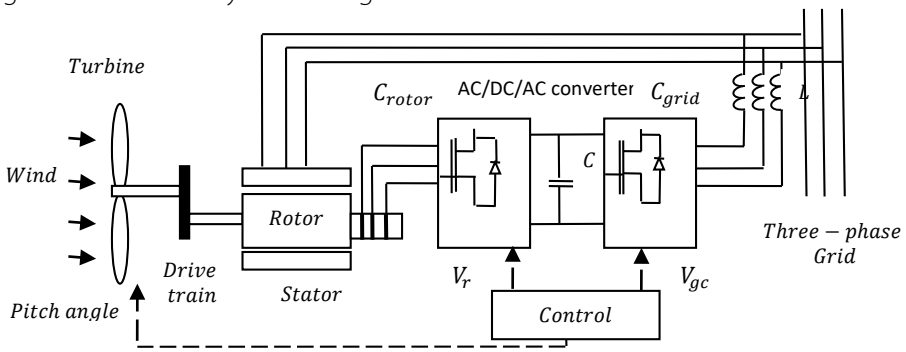


Figure 1. Wind turbine with doubly fed induction generator

The control system generates the pitch angle command and $\mathbf{V_r}$ and $\mathbf{V_{gc}}$ control voltage signals for $\mathbf{C_{rotor}}$ and $\mathbf{C_{grid}}$, in order to control wind turbine power, $\mathbf{DC}$ bus voltage and reactive power or voltage at the grid terminals. The wind power captured by the wind turbine is converted into electrical power by the induction

generator and transferred to the grid by stator and rotor windings. The aerodynamic torque generated by the wind turning the turbine blades, is expressed as follow:

$$T_a = \frac{1}{2\omega_r}\rho A V^3 C_p(\lambda,\beta) \tag{1}$$

where $A = \pi R^2$ is the area swept by the turbine blades, $R$ is the blade radius, $C_p(\lambda,\beta)$ is the power coefficient depending on $\lambda = R\omega_r/V$ the ratio of rotor speed ($R\omega_r$) and wind speed $V$, respectively.
The power coefficient $C_p(\lambda,\beta)$ is determined with expressions given in [18].
For modeling the drivetrain, the configuration shown in Figure 2 is considered.

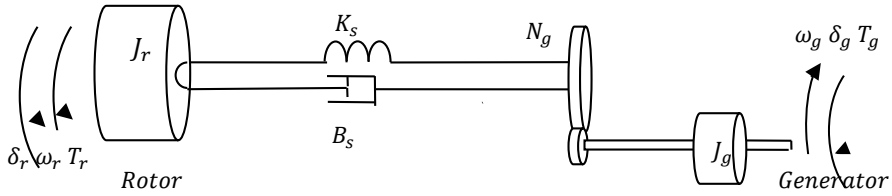


Figure 2. Drivetrain configuration

Applying the torque equilibrium laws, the transmission system is described by the following equations [17]:

$$\begin{gathered} J_r\dot{\omega}_r = T_r - T_s = T_a - K_s\delta - B_s\left(\omega_r - \frac{\omega_g}{N_g}\right);\ \dot{\delta} = \omega_r - \frac{\omega_g}{N_g};\\ N_g J_g\dot{\omega}_g = T_s - T_g N_g = K_s\delta + B_s\left(\omega_r - \frac{\omega_g}{N_g}\right) - T_g N_g \end{gathered} \tag{2}$$

where $J_r, J_g$ are the moments of inertia of the rotor and generator; $\omega_r, \omega_g$ are the rotor and generator speeds; $B_s, K_s$ are the damping and stiffness coefficients of the drivetrain, $\delta$ is the drivetrain torsion and $N_g$ is the gearbox ratio.
The equation system (2) is nonlinear, as the torque $T_r = T_a$ is acting on the rotor.
For $\omega_r$ , $\delta$, $\omega_g$ are considered small variations around a static operating point, corresponding to a stationary behavior, $\Delta x = x - x_0$ . The state variables are introduced:

$$x_1 = \Delta\omega_r = \omega_r - \omega_{r0};\ x_2 = \Delta\delta = \delta - \delta_0;\ x_3 = \Delta\omega_g = \omega_g - \omega_{g0} \tag{3}$$

The variation of the torque $T_a$ is given by the expression:

$$\begin{gathered} \Delta T_a = T_a - T_{a0} = \left.\frac{\partial T_a}{\partial\omega_r}\right|_{\omega r0}\Delta\omega_r + \left.\frac{\partial T_a}{\partial V}\right|_{V0}\Delta V + \left.\frac{\partial T_a}{\partial\beta}\right|_{\beta 0}\Delta\beta =\\ \left.\frac{\partial T_a}{\partial\omega_r}\right|_{\omega r0} x_1 + \left.\frac{\partial T_a}{\partial\beta}\right|_{\beta 0}\Delta\beta + \left.\frac{\partial T_a}{\partial V}\right|_{V0}\Delta V = a_r x_1 + b_r\Delta\beta + c_r\Delta V \end{gathered} \tag{4}$$

Taking into account relations (3) and (4) the following linear state space model of the drivetrain is obtained:

$$\begin{bmatrix}\dot{x}_1\\ \dot{x}_2\\ \dot{x}_3\end{bmatrix} = \begin{bmatrix}\frac{a_r - B_s}{J_r} & -\frac{K_s}{J_r} & \frac{B_s}{N_g J_r}\\ 1 & 0 & -\frac{1}{N_g}\\ \frac{B_s}{N_g J_g} & \frac{K_s}{N_g J_g} & -\frac{B_s}{N_g^2 J_g}\end{bmatrix}\begin{bmatrix}x_1\\ x_2\\ x_3\end{bmatrix} + \begin{bmatrix}\frac{c_r}{J_r} & \frac{b_r}{J_r} & 0\\ 0 & 0 & 0\\ 0 & 0 & -\frac{1}{J_g}\end{bmatrix}\begin{bmatrix}\Delta V\\ \Delta\beta\\ \Delta T_g\end{bmatrix} \tag{5}$$

where $x = [x_1 \quad x_2 \quad x_3]^T$ the state vector and $u = [\Delta V \quad \Delta\beta \quad \Delta T_g]^T$ the input vector, with $\Delta V$- the perturbation of the system and $\Delta\beta$ , $\Delta T_g$ - the control variables. The output of the wind turbine: generator speed variation $y_1 = \Delta\omega_g = x_3$ and the generator power variation $y_2 = \Delta P = T_{g0}\Delta\omega_g + \omega_{g0}\Delta T_g = T_{g0}x_3 + \omega_{g0}\Delta T_g$ . Also, let's note $A$ - state matrix, $B$ - input matrix and $C$ - output matrix.
A characteristic equation for wind turbine drive system is obtained by calculating the determinant $\Delta(s)$ of the matrix $(sI - A)$:

$$\Delta(s) = s^3 + s^2\left(-\frac{a_r}{J_r} + B_s\frac{J_t}{N_g^2 J_r J_g}\right) + s\left(-\frac{a_r B_s}{N_g^2 J_r J_g} + \frac{K_s J_t}{N_g^2 J_r J_g}\right) - \frac{a_r K_s}{N_g^2 J_r J_g} = 0 \tag{6}$$

The characteristic equation can be approximated with the following factorized form:

$$\begin{gathered} \Delta(s) = (s+a)(s^2 + bs + c) = 0\\ a = -\frac{a_r}{J_t},\ b = \frac{B_s J_t}{N_g^2 J_r J_g} - \frac{a_r}{J_r} + \frac{a_r}{J_t},\ c = \frac{K_s J_t}{N_g^2 J_r J_g} - \frac{a_r^2}{J_r J_t} + \frac{a_r^2}{J_t^2};\ J_t = J_r + N_g^2 J_g \end{gathered} \tag{7}$$

The transfer function is defined as:

$$H_\beta(s) = \frac{\Delta\omega_g(s)}{\Delta\beta(s)} = \frac{b_r}{N_g J_r J_g} \frac{B_s s + K_s}{(s+a)(s^2+bs+c)} \quad (8)$$

The pitch angle is controlled using a servo system with three types of control loop- position, velocity and torque. The pitch angle actuator is considered to be described by a 2nd order model [18]:

$$H_a(s) = \frac{\omega_a^2}{s^2 2\xi_a\omega_a s + \omega_a^2} \quad (9)$$

where $\omega_a$ is the natural frequency and $\xi_a$ is the damping factor for the pitch actuator subsystem. Thus, the process transfer function can be written:

$$H_p(s) = H_\beta(s)H_a(s) \quad (10)$$

A PID controller with the following transfer function can be used for speed control of generator system:

$$H_{c\,PID}(s) = K_p + \frac{K_i}{s} + K_d s \quad (11)$$

where $K_p, K_i, K_d$ are the proportional, integral and derivative gains.

## 3. REQUIREMENTS FOR $H_\infty$ DESIGN CONTROLLERS

For the $H_\infty$ robust controller design, it was considered the model schematically shown in Figure 3. Here, the weighted process $P$ consist in: the transfer matrix $H_p(s)$ of the real process, the weighting functions $W_1(s), W_2(s), W_3(s)$ of tracking error $e$, control input $u$ (include $r$-reference input), output $y$ (response) and $H_c$ controller of the system. By $u_1$ and $u_2$ were denoted the inputs of the weighted process $P(s)$, and by $y_1$ and $y_2$ were denoted its outputs, where: $u_1 = [r \quad n]^T$, $u_2 = u$; $y_1 = [y_{11} \quad y_{12} \quad y_{13}]^T$; $y_2 = e$.

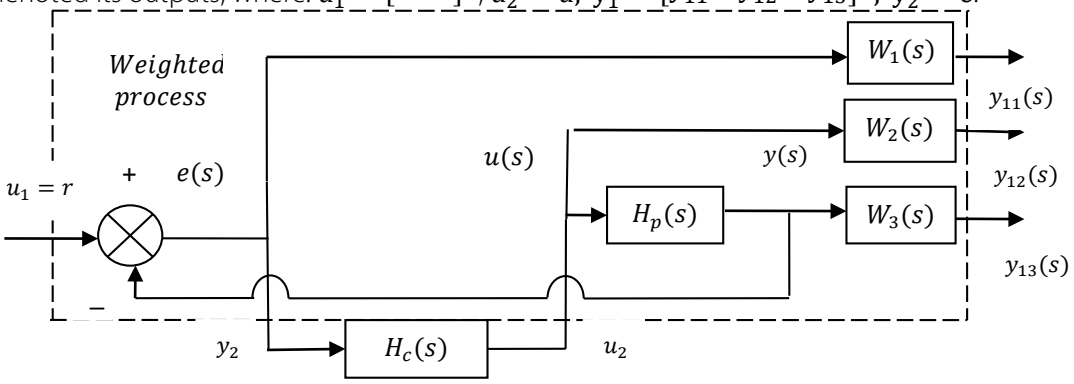


Figure 3. Weighted process control block diagram

The weighted process $P(s)$ can be written as a function of the nominal process $H_p(s)$ and the weighting matrices $W_1(s)$, $W_2(s)$, and $W_3(s)$:

$$P(s) = \begin{bmatrix} W_1(s) & | & -W_1(s)H_p(s) \\ 0 & | & W_2(s) \\ 0 & | & W_3(s)H_p(s) \\ -- & - & ----- \\ I & | & -H_p(s) \end{bmatrix} = \begin{bmatrix} P_{11}(s) & P_{12}(s) \\ P_{21}(s) & P_{22}(s) \end{bmatrix} \quad (12)$$

The closed loop transfer function or the cost function defines the transfer from inputs $u_1$ to outputs $y_1$ and is expressed as a linear fractional transformation $F_l(P, H_c)$:

$$T_{y1u1}(s) = F_l(P, H_c) = P_{11} + P_2 H_c (I - P_{22}H_c)^{-1} P_{21} \quad (13)$$

Taking into account the sensitivity functions $S(s), T(s)$ and $R(s)$ defined by:

$$S(s) = [I + H_c(s)H_p(s)]^{-1}$$
$$T(s) = H_c(s)H_p(s)\,S(s); \quad R(s) = H_p(s)\,S(s) \quad (14)$$

The cost function of the weighted process control system can be written as:

$$T_{y1u1}(s) = \begin{bmatrix} W_1(s)S(s) \\ W_2(s)R(s) \\ W_3(s)T(s) \end{bmatrix} \quad (15)$$

The $H_\infty$ controller synthesis problem can be formulated as follows: knowing the weighted process $P(s)$ find a controller described by the transfer matrix $H_c(s)$ that realizes the control law:

$$U_2(s) = -H_c(s)Y_2(s) \quad (16)$$

such that the norm $H_\infty$ of the cost function $T_{y1u1}$ is minimized $\min\|T_{y1u1}\|_\infty$.

The $H_\infty$ norm of a given system $H(s)$ is defined in terms of singular values $\sigma_i(H(j\omega)),\ i = 1,2 \ldots n$:

$$\|H\|_\infty = \sup_{\omega\in\Re} \bar{\sigma}(H(j\omega)) \tag{17}$$

where $\bar{\sigma}$ is the maximum singular value. The singular values are a measure of gain for an $H$ system.
The weighting functions $W_1(s)$, $W_2(s)$ and $W_3(s)$ are defined by [20]:

$$W_1(s) = \frac{\frac{s}{M_s}+\omega_b}{s+\omega_b\varepsilon_1} \;;\; W_2(s) = \frac{s+\frac{\omega_{b0}}{M_u}}{\varepsilon_2 s+\omega_{b0}} \;;\; W_3(s) = \frac{s+\frac{\omega_{c0}}{M_T}}{\varepsilon_3 s+\omega_{c0}} \tag{18}$$

where $\omega_b$ is the frequency bandwidth of the open system, and $M_s$ is the peak of the sensitivity function $S(s)$ ; $\omega_{bc}$ is the bandwidth of the controller, $\omega_{b0}$ is the bandwidth of the closed loop, $M_u$ is the peak of $R(j\omega)$, $M_T$ is the peak of $T(j\omega)$, and $\varepsilon_2$ ,$\varepsilon_3$ have small values.
The performance of a closed loop system can be specified by:

$$|S(j\omega)| \le \varepsilon\,, \forall\,\omega \le \omega_b \;;\; |S(j\omega)| \le M_s\,, \forall\,\omega > \omega_b \tag{19}$$

In the case of monovariable (SISO -Single Input Single Output) or multivariable (MIMO -Multiple Input Mutiple Output) systems, the performance specifications are described by the relations:

$$\sigma_i(S(j\omega)) \le \bar{\sigma}\big(S(j\omega)\big) \le \left|W_1^{-1}(j\omega)\right| ;\; |S(j\omega)| \le \left|W_1^{-1}(j\omega)\right| \tag{20}$$

Robust stability conditions can be expressed in the frequency domain using the weighting functions $W_2(s)$ and $W_3(s)$ and the sensitivity matrices $R(s)$ and $T(s)$:

$$\bar{\sigma}\big(R(j\omega)\big) \le \left|W_2^{-1}(j\omega)\right| ;\; \bar{\sigma}\big(T(j\omega)\big) \le \left|W_3^{-1}(j\omega)\right| \tag{21}$$

In the case of additive disturbances, $W_2(j\omega)$ acts as a filter on $R(j\omega)$ and penalizes the command, $u$. In the case of multivariable disturbances $W_3(j\omega)$ weights the complementary sensitivity, $T(j\omega)$, thus penalizing the system output.
The calculation of the $H_\infty$ controller can be obtained by using the Riccati equations approach or the LMI (linear matrix inequalities) approach [11].
The $H_\infty$ control problem can be solved by mixed sensitivity method (mixsyn) using the expression:

$$\left\|T_{y1u1}\right\|_\infty = \left\|[W_1S, W_2R, W_3T]^T\right\|_\infty \le \gamma \tag{22}$$

where $\gamma = GAM$ is a positive number $\gamma > 0$.
On consider $H_p(s)$, the process control system, weighted by the functions $W_1(s)$, $W_2(s)$, $W_3(s)$. If expression (22) of the cost function is used, the $H_\infty$ problem can be solved by the misxyn method of sensitivities [10], using the following Matlab command:

$$[K, CL, GAM, INFO] = \text{mixsyn}(H_p, W_1, W_2, W_3) \tag{23}$$

which computes a controller $K$ that minimizes the $H_\infty$ norm of the weighted closed-loop transfer function $T_{y1u1}(s)$.

## 4. MATHEMATICAL MODELING AND VECTOR CONTROL OF DOUBLY FED INDUCTION GENERATOR

For stator and rotor variables, the subscripts $s$ (e.g. $u_{ds}$ , $\varphi_{qs}$) –for stator and $r$ (e.g. $u_{qr}$ , $\varphi_{dr}$) – for rotor were used. The notations used are as follow : $u_d$ , $u_q$– for voltages, $i_d$, $i_q$– for currents ,$\varphi_d$ , $\varphi_q$ – for magnetic fluxes , $R_s, R_r$ and $L_s, L_r$ - for stator and rotor resistances and inductances, $L_m$ – mutual inductance, $\omega_s$– angular velocity at synchronism, $\omega_r$– angular velocity of the rotor, $\Omega_r$– mechanical angular velocity of the rotor, $p$ – number of pairs of poles; $\omega_r = p\Omega_r$ .
The equations describing the DFIG model, in $(d-q)$ frame are as follows [8], [13], [16]:

$$\begin{cases} u_{ds} = R_s i_{ds} + \frac{d}{dt}\varphi_{ds} - \omega_s\varphi_{qs} \\ u_{qs} = R_s i_{qs} + \frac{d}{dt}\varphi_{qs} + \omega_s\varphi_{ds} \\ u_{dr} = R_r i_{ds} + \frac{d}{dt}\varphi_{dr} - (\omega_s-\omega_r)\varphi_{qr} \\ u_{qr} = R_r i_{qs} + \frac{d}{dt}\varphi_{qr} + (\omega_s-\omega_r)\varphi_{dr} \end{cases} ; \quad \begin{cases} \varphi_{ds} = L_s i_{ds} + L_m i_{dr} \\ \varphi_{qs} = L_s i_{qs} + L_m i_{qr} \\ \varphi_{dr} = L_r i_{dr} + L_m i_{ds} \\ \varphi_{qr} = L_r i_{qr} + L_m i_{qs} \end{cases} \tag{24}$$

The vector control strategy divides the DFIG model into two independent subsystems, torque and flux, in order to achieve similar performance to $DC$ motor speed control. Thus, if the stator flux $\varphi_s$ is chosen to be oriented along the direct axis (d) in the Park reference system [3], [6] :

$$\varphi_{ds} = \varphi_s,\; \varphi_{qs} = 0 \tag{25}$$

If the stator resistance in each phase is neglected, assuming that the stator flux is constant, it can be written:

$$u_{ds} = 0, u_{qs} = u_s = \omega_s\varphi_s \tag{26}$$

Consequently, the electromagnetic torque and the active and reactive powers are determined by:

$$T_{em} = -p\omega_s\frac{L_m}{L_s}i_{qr} \Rightarrow i_{qr} = -\frac{L_s}{p\omega_s L_m}T_{em} \tag{27}$$

$$P_s = -u_s \frac{L_m}{L_s} i_{qr},\ \ Q_s = \frac{u_s^2}{\omega_s L_s} - u_s \frac{L_m}{L_s} i_{dr} \Rightarrow i_{dr} = \left(Q_s - \frac{u_s^2}{\omega_s L_s}\right)\left(\frac{L_s}{u_s L_m}\right)$$

Also, the equations for rotor voltages can be expressed as:

$$\begin{gathered} u_{dr} = R_r i_{dr} + \sigma \frac{di_{dr}}{dt} - s_a \sigma \omega_s i_{qr} \\ u_{qr} = R_r i_{qr} + \sigma \frac{di_{qr}}{dt} + s_a \sigma \omega_s i_{dr} + s_a \frac{u_s L_m}{L_s};\ \sigma = \frac{L_s L_r - L_m^2}{L_s};\ s_a = \frac{(\omega_s - \omega_g)}{\omega_s} \end{gathered} \quad (28)$$

Applying Laplace transform to equations (28) it can be obtain:

$$\begin{gathered} u_{dr}(s) = (R_r + s\sigma) i_{dr}(s) - s_a \sigma \omega_s i_{rq}(s) \\ u_{qr}(s) = (R_r + s\sigma) i_{rq}(s) - s_a \sigma \omega_s i_{rd}(s) + s_a \frac{u_s L_m}{L_s} \end{gathered} \quad (29)$$

In the case of the vector control strategy, the system performance depends on the generator parameters, and in particular on the rotor resistance. When the parameters of the control system change due to temperature variation or saturation, the system performance degrades.

To solve this problem, convetional proportional-integral PI controllers are replaced by FOPI controllers [6]. A fractional order controller increases robustness and improves system performance wih the additional parameter $\lambda$, which represents the fractional order of the integrating action. The use of this controller leads to good dynamic performance and robustness of the DFIG under both normal and critical conditions.

The transfer functions of the two controllers, **PI** and **FOPI** can be written as follows [2], [9], [15]:

$$H_{PI}(s) = K_p\left(1 + \frac{K_i}{s}\right);\ H_{FOPI}(s) = K_p\left(1 + \frac{K_i}{s^\lambda}\right) \quad (30)$$

where $K_p$ , $K_i$ and $\lambda$ are real numbers, $\lambda \in [0,1]$.

Based on equations (24) and (25) - (30), the proposed DFIG control scheme based on two fractional-order controllers $H_{FOPI}$, shown in Figure 4, is realized. In this scheme, two current control loops appear, $i_{dr}$ and $i_{qr}$ . The loops are interconnected by blocks $s_a \omega_s \sigma$.

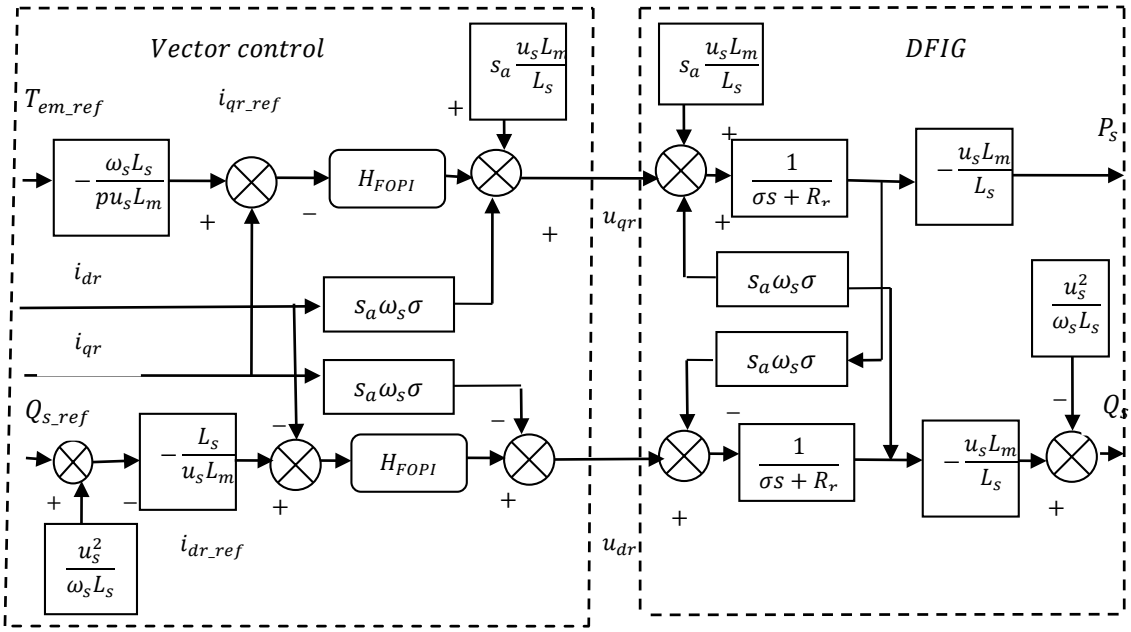


Figure 4. DFIG generator control scheme

The active $P_s$ and reactive $Q_s$ power control of the DFIG generator is achieved by controlling two monovariable first-order linear subsystems with two **PI** or **FOPI** controllers.

Typically, DFIG is controlled using the vector control strategy, with either flux or voltage orientation. By this method, the nonlinear MIMO system of the DFIG is divided into two linear SISO systems, separately representing the rotor currents [2], [3], [6]. By controlling two components of rotor it is possible to independently control the active and reactive power of the generator. In order to compensate for the variations of the generator parameters in two single variable systems, conventional proportional integral **PI** controllers are replaced by **FOPI** controllers.

— Fractional order FOPI controller design for current loop of DFIG generator

Consider the current loops uncoupled. In this case, the current loop $i_{qr}$ is shown in Figure 5.

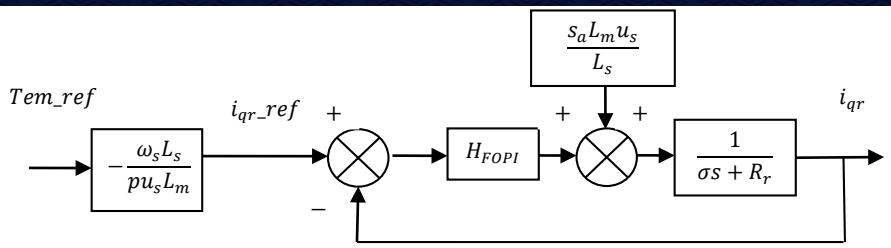


Figure 5. Loop for current control $\mathbf{i_{qr}}$

The process has the transfer function:

$$\mathrm{H(s)} = \frac{\mathrm{K}}{1+\mathrm{Ts}} = \frac{1}{\sigma \mathrm{s} + \mathrm{R_r}} = \frac{{}^{1}/_{\mathrm{R_r}}}{{}^{\sigma}/_{\mathrm{R_r}}\,\mathrm{s}+1};\ \mathrm{K} = \frac{1}{\mathrm{R_r}};\ \ \mathrm{T} = \frac{\sigma}{\mathrm{R_r}} \tag{31}$$

It is proposed to implemnet a FOPI controller. The parameters of the generator are considered to have the following values : $\mathrm{L_s} = 0.0137\ \mathrm{H}\,;\mathrm{L_r} = 0.0136\ \mathrm{H}\,;\ \ \mathrm{L_m} = 0.0135\ \mathrm{H};\ \mathrm{R_r} = 0.021\ \Omega$.
Determine the parameters K and T, as follows:

$$\sigma = \mathrm{L_r} - \frac{\mathrm{L_m^2}}{\mathrm{L_s}} = 0.0003;\ \mathrm{K} = \frac{1}{\mathrm{R_r}} = 47.619\,;\mathrm{T} = \frac{\sigma}{\mathrm{R_r}} \cong 0.0143 \tag{32}$$

In the following we consider the transfer functions of the process $\mathrm{H(s)}$, the fractional order controller $\mathrm{H_{FOPI}(s)}$ and the open loop system $\mathrm{H_d(s)}$:

$$\mathrm{H(s)} = \frac{\mathrm{K}}{1+\mathrm{Ts}} = \frac{47.619}{1+0.0143\mathrm{s}};\ \mathrm{H_{FOPI}(s)} = \mathrm{K_p}\left(1+\frac{\mathrm{K_i}}{\mathrm{s}^{\lambda}}\right);\ \lambda \in (0,1) \tag{33}$$
$$\mathrm{H_d(s)} = \mathrm{H_{FOPI}H(s)}$$

The open loop transfer function for an integer-order PI controller is expressed as:

$$\mathrm{H_d(s)} = \mathrm{K_p}\left(1+\frac{\mathrm{K_i}}{\mathrm{s}}\right)\frac{\mathrm{K}}{\mathrm{Ts}+1} \tag{34}$$

— FOPI controller design requirements

In order to ensure the stability and robustness of the system, restrictions are imposed on the controller design, namely [15], [19]:

a) Phase margin specification:

$$\arg[\mathrm{H_d(j\omega_c)}] = \arg[\mathrm{H_{FOPI}(j\omega_c)H(j\omega_c)}] = -\pi + \varphi_{\mathrm{m}} \tag{35}$$

where $\mathrm{H_d(j\omega)}$ is the transfer function of the open loop system, and $\omega_c$ is the cut-off frequency.

b) Restriction on magnitude at cut-off frequency:

$$|\mathrm{H_d(j\omega_c)}|_{\mathrm{dB}} = |\mathrm{H_{FOPI}(j\omega_c)H(j\omega_c)}|_{\mathrm{dB}} = 0 \tag{36}$$

c) Robustness to variation in the gain, that is the derivative of the phase of the open-loop system with respect to the frequency is forced to be zero at the gain crossover frequency, thus:

$$\left.\frac{\mathrm{d}\left(\arg \mathrm{H_d(j\omega_c)}\right)}{\mathrm{d}\omega}\right|_{\omega=\omega_c} = 0 \tag{37}$$

## 5. DESIGN AND SIMULATION RESULTS IN MATLAB

For the controller design, a wind turbine with a power of $1.5\ \mathrm{MW}$ was considered with parameters: the moment of inertia of the turbine rotor $\mathrm{J_r} = 3.605\mathrm{e}+06\ \mathrm{kgm^2}$, the moment of inertia of the generator $\mathrm{J_g} = 93.628\ \mathrm{kgm^2}$, stiffness coefficient of the drivetrain $\mathrm{K_s} = 3.03\mathrm{e}+08\ \mathrm{Nm/rad}$, damping coefficient of the drivetrain $\mathrm{B_s} = 1.72\mathrm{e}+05\ \mathrm{Nm/s}$ and gearbox ratio $\mathrm{N_g} = 95$.

The resulting process transfer function : $\mathrm{H_p(s)} = \frac{0.0077\mathrm{s}+13.56}{\mathrm{s}^5+17.20\mathrm{s}^4+165.79\mathrm{s}^3+1004.5\mathrm{s}^2+4713.2\mathrm{s}+9022.3}$.

The linearized turbine model was considered around the operating point corresponding to the nominal wind speed $\mathrm{Vw_0} = 10\mathrm{m/s}$. The coefficients $\mathrm{a_r} = -1.496\mathrm{e}+07$, $\mathrm{b_r} = 22.423$, $\mathrm{c_r} = 12.625\mathrm{e}+04$ were determined.

For the sensitivity functions $\mathrm{S}$ and $\mathrm{T}$, the frequencies $\omega_0 = 15\ \mathrm{rad/s}$ , $\omega_b = 30\ \mathrm{rad/s}$ and modulus $\mathrm{M} = 1.9$ were considered.

For the synthesis of the $\mathrm{H_\infty}$ controllers the $\mathbf{mixsyn}$ function was used. For the specifications design the functions $\mathrm{W_1(s)}$ and $\mathrm{W_3(s)}$ are determinate which penalize the error $\mathbf{e}$ and the output $\mathbf{y}$.

Figure 6 shows the singular values for $\mathrm{W_1^{-1}(j\omega)}$ and $\mathrm{W_3^{-1}(j\omega)}$. The singular value of the cost function $\mathrm{T_{u1y1}(j\omega)}$ obtained with $\mathrm{H_\infty}$ controller is shown in Figure 7. In Figure 8 are illustrated the singular value for both, sensitivity function $\mathrm{S}$ and ${}^{\mathrm{GAM}}/_{\mathrm{W_1}}$. It can be observed that the inequality $\overline{\sigma}(\mathrm{s}) \le \frac{\mathrm{GAM}}{|\mathrm{W_1(j\omega)}|}$ is satisfied.

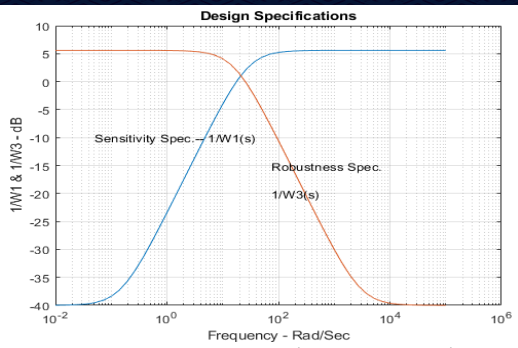


Figure 6. Singular values for $W_1^{-1}(j\omega)$ and $W_3^{-1}(j\omega)$

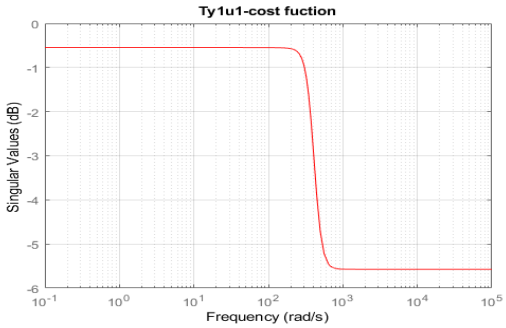


Figure 7. Singular value of the cost function $T_{u1y1}$

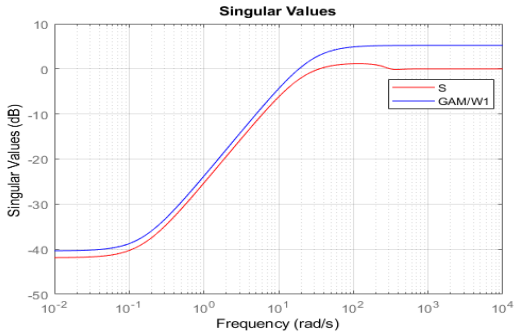


Figure 8. The singular value of the sensitivity function S and $GAM/W_1$

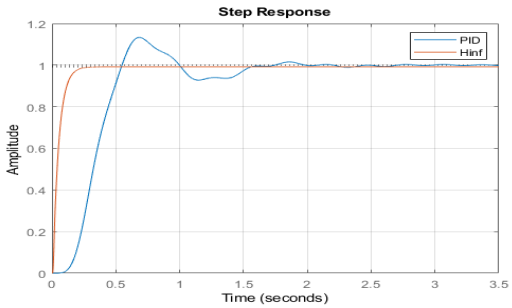


Figure 9. Step responses of the control loop for PID and $H_\infty$ controller

For the PID controller, the proportional gain $K_p = 8.56e+03$, the integral gain $K_i = 2.21e+04$ and the derivative gain $K_d = 191$ were determined with the PIDtune function from Matlab program.

Figure 9 shows the closed loop responses for a PID controller and $H_\infty$, respectively. Comparing these responses with the step response obtained with an $H_\infty$ controller shows the superiority of this controller. An aperiodic response and a very short response time are obtained.

Using relations (31), (32) and the values of the determined parameters, the Simulink model of FOPI controller is illustrated in Figure 10.

The step responses of the current loops are displayed for a simulation time of $0.15$ seconds. The gain of process is considered to be $K = \frac{1}{Rr}, \frac{0.5}{R_r}$ and $2R_r$. The results obtained are illustrated in Figure 11.

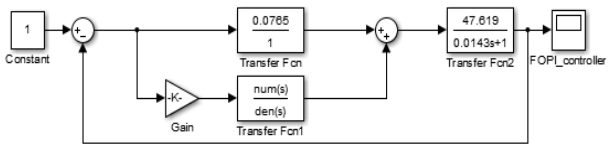


Figure 10. Simulink model of FO$PI$ controller

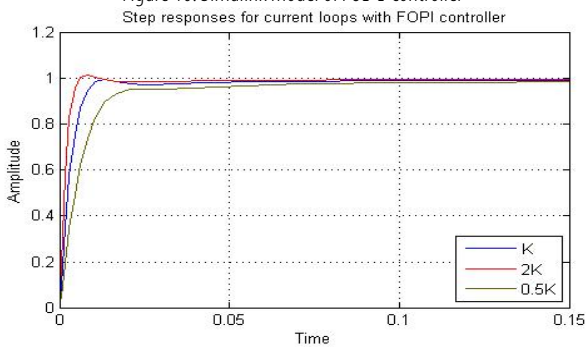


Figure 11. Step responses- current loops with $FOPI$ controller

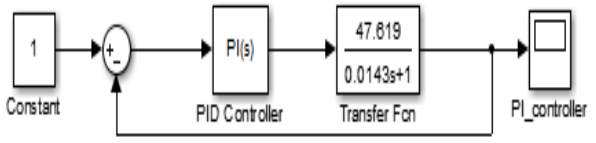


Figure 12. Simulink model using an integer order $PI$ controller

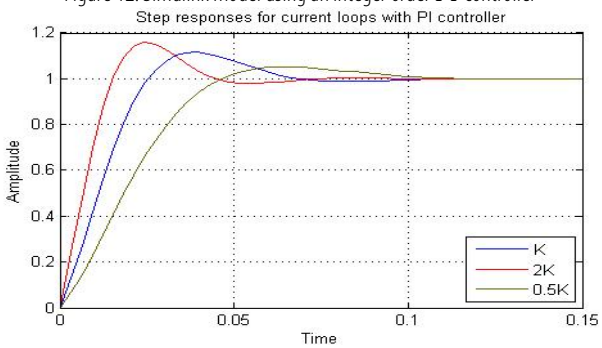


Figure 13. Step responses- current loops with $PI$ controller

Figure 12 shows the Simulink model for a conventional PI controller. The simulations were performed for $0.15$ seconds and for a gain of process $K = \frac{1}{Rr}, \frac{0.5}{R_r}$ and $2R_r$. The step response of the system can be seen in Figure 13.

## 6. CONCLUSIONS

In this paper a $H_\infty$ controller for drivetrain control and a FOPI controller for controlling the currents of the doubly fed induction generator were designed. The design and application details of $H_\infty$ and FOPI controllers are discussed.

For the $H_\infty$ synthesis method, the transfer function of the process was determined and weighting functions were introduced to satisfy the design specifications. Therefore, for the $H_\infty$ synthesis the mixsyn function in Matlab program was used.

For the generator control, the vector control strategy was applied, which provides decoupling between torque and flux.

For comparison, two conventional controllers were designed, namely a PID controller for the drivetrain and a PI controller for control the current loops of DFIG generator.

Simulation results shows that by using the two proposed controllers, higher performance is achieved compared to conventional controllers.

**Note**: This paper was presented at XX$^{th}$ National Conference on Electric Drives – CNAE 2021/2022, organized by the Romanian Electric Drive Association and the Faculty of Electrotechnics and Electroenergetics –University Politechnica Timisoara, in Timisoara (ROMANIA), between May 12–14, 2022 (initially scheduled for October 14–16, 2021).

## References

[1] Arifujjaman, M.; Iqbal, M.T.; Quaicoe, J.E. : Vector Control of a DFIG Based Wind Turbine, Journal of Electrical and Electronics Engineering, Vol. 9 (No.2), 2009.
[2] Azza, A.; Kherfane H.: Robust Control of Doubly Fed Induction Generator Using Fractional Order Control, International Journal of Power Electronics and Drive System, Vol. 9 (No. 3), pp.1072-1080, September 2018.
[3] Becheri, H.; Bousserhane, I. K.; Bouchiba, B. ; Harrouz, A.; Belbekri, T. : Vector Control of Wind Turbine Conversion chain Variable Speed Based on DFIG Using MPPT Strategy, International Journal of Applied Engineering Research, Vol.13 (No. 7), 2018.
[4] Bhattacharyya, S. P.: Robust control under parametric uncertainty: An overview and recent results, Annual Reviews in Control, Vol 44, pp 45-77, 2017.
[5] Boubzizi, S.; Abid, H.; El Hajjaji, A.; Chaabane, M.: Comparative study of three types of controllers for DFIG in wind energy conversion system, Protection and Control of Modern Power Systems, 2018.
[6] Bounifli, F.E.; El Moudden, A.; WAHABI, A.; Hmidat, A.: Vector Control of a Doubly-Fed Induction Generator by Using a Classical PI and a fuzzy PI Controllers, World Journal of Innovative Research, Vol. 1 (No. 2), pp. 18-24, December 2016.
[7] Chen, Y. Q.; Petras, I.; Xue, D.: Fractional Order Control - A Tutorial, American Control Conference, USA, 2009.
[8] Ezzahi, M.; Khafallah, M.; Majid, F.: Sub-synchronous and hyper-synchronous modeling of Doubly Fed Induction Generator (DFIG) through a Field Oriented Control (FOC), The second International Conference on Smart Applications and Data Analysis for Smart Cities, 2018.
[9] Faieghi, M. R. ; Nemati, A.: On Fractional-Order PID Design, Applications of Matlab in Science and Engineering, Ed. InTech, 2011.
[10] Gilev, B.: Mixed Sensitive Controller Design for Wind Turbine, Proceedings of the 44th Conference on Applications of Mathematics in Engineering and Economics, AIP Conference Proceedings 2048, 020002-1-020002-8, 2018.
[11] Haneesh, K.M.; Raghunathan, T.: Robust Control of DIFG Based Wind Energy System Using an $H_\infty$ Controller, Journal of Electrical Engineering & Technology, Published Online: 25 March 2021.
[12] Kaloi, G. S.; Wang, J.; Baloch, M. H.: Active and reactive power control of the doubly fed induction generator based on wind energy conversion system, Energy Reports, Vol 2, pp 194-200, 2016.
[13] Kasbi, A.; Rahali, A.: Design a Fractional Order Controller for Power Control of Doubly Fed Induction Generator Based Wind Generation System, International Journal of Energy and Power Engineering, Vol. 13( No. 8), 2019.
[14] Livint, G.; Baciu, A. G.: Sisteme de control robust, Ed. Matrix Rom, Bucuresti, 2020.
[15] Monje, A.; Chen, Y.Q.; Vinagre, B.M.; Xue, D.; Feliu, V.: "Fractional-order systems and controls", Springer, 2010.
[16] Nadour, M.; Essadki, A.; Nasser, T.: Comparative Analysis between PI & Backstepping Control Strategies of DFIG Driven by Wind Turbine, International Journal of Renewable Energy Research, Vol. 7 (No. 3), 2017.
[17] Popescu, D.; Ionescu, F.; Dobrescu, R.; Stefanoiu, D.: Modelare in ingineria proceselor industriale, Ed. AGIR, Bucuresti 2011.
[18] Poureh, A.; Nobakhti, A.: Robust control design for an industrial wind turbine with HIL simulations, ISA Transactions, Vol 103, pp 252-265, 2020.
[19] Razaei, V.: Advanced of Wind Turbines: Brief Survey, Categorization, and Challenges, American Control Conference, IL, USA, July 2015.
[20] Yuan, Y.; Chen, X.; Tang, J.: Multivariable robust blade pitch control design to reject periodic loads on wind turbines, Renewable Energy, Vol 146, pp 329-341, 2020.



ISSN 1584 – 2665 (printed version); ISSN 2601 – 2332 (online); ISSN-L 1584 – 2665